Editors' Suggestion | Featured in Physics

RETRACTED: Synthesis of Yttrium Superhydride Superconductor with a Transition Temperature up to 262 K by Catalytic Hydrogenation at High Pressures

Elliot Snider,[1,†] Nathan Dasenbrock-Gammon,[2,†] Raymond McBride,[1] Xiaoyu Wang,[3] Noah Meyers,[1] Keith V. Lawler,[4] Eva Zurek,[3] Ashkan Salamat,[5] and Ranga P. Dias[1,2,*]

[1]*Department of Mechanical Engineering, School of Engineering and Applied Sciences, University of Rochester, Rochester, New York 14627, USA*

[2]*Department of Physics and Astronomy, University of Rochester, Rochester, New York 14627, USA*

[3]*Department of Chemistry, State University of New York at Buffalo, Buffalo, New York 14260, USA*

[4]*Department of Chemistry & Biochemistry, University of Nevada Las Vegas, Las Vegas, Nevada 89154, USA*

[5]*Department of Physics & Astronomy, University of Nevada Las Vegas, Las Vegas, Nevada 89154, USA*

(Received 17 November 2020; accepted 19 January 2021; published 19 March 2021)

The recent observation of room-temperature superconductivity will undoubtedly lead to a surge in the discovery of new, dense, hydrogen-rich materials. The rare earth metal superhydrides are predicted to have very high-T_c superconductivity that is tunable with changes in stoichiometry or doping. Here we report the synthesis of an yttrium superhydride that exhibits superconductivity at a critical temperature of 262 K at 182 ± 8 GPa. A palladium thin film assists the synthesis by protecting the sputtered yttrium from oxidation and promoting subsequent hydrogenation. Phonon-mediated superconductivity is established by the observation of zero resistance, an isotope effect and the reduction of T_c under an external magnetic field. The upper critical magnetic field is 103 T at zero temperature.

DOI: 10.1103/PhysRevLett.126.117003

Metallic hydrogen is considered to have a high Debye temperature and strong electron-phonon coupling that is necessary for high T_c phonon-mediated superconductivity [1–4]. Based on the properties of metallic hydrogen [5,6], metal hydride compounds have long been investigated as a means toward increasing T_c via the hydrogen acting as a "superconducting glue" providing high frequency vibrations [7], but early metal hydride studies were unable to achieve T_cs over 20 K [8]. The discovery of superconductivity in hydrogen sulfide at 203 K changed the notion of what might be possible for phonon-mediated superconductors [9–12]. This has been further supported by our own report of room temperature superconductivity (RTSC) in a carbonaceous sulfur hydride [13]. The resulting paradigm shift has cemented the understanding that a hydride compound must have a large electron-phonon coupling related to the hydrogen atoms and a high density of hydrogen related states at the Fermi level (only achieved by forms of hydrogen other than H_2, H^-, H_3^-) to have a high T_c [14]. High hydrogen content materials that meet those two criteria can be considered as chemically precompressed phases relative to pure hydrogen, thus lowering the pressures necessary for metallization or high T_c superconductivity to more experimentally feasible conditions [15].

High T_c hydrogen-rich materials can be broadly categorized into two types: purely covalent metallic hydrides, such as hydrogen sulfide and the newly discovered RTSC carbonaceous sulfur hydride [13], and the so-called metal "superhydrides." In the later metal superhydrides, metal atoms occupy the center of the cages of clathratelike hydrogen lattices [14,16–21]. Predictions for many metal superhydrides are exceptionally encouraging for achieving unprecedented T_cs—the theoretical work on the lanthanum and yttrium superhydrides thus far has suggested T_c values of 274–286 K at 210 GPa and reaching as high as 305–326 K at 250 GPa [22]. Interestingly, scandium (the lightest rare earth) has been predicted to exhibit a range of superhydride stoichiometries with superconducting properties and exotic hydrogen bonding networks [23] that are unique compared to those of Y and La, indicating an ion-size effect. Somewhat counterintuitively, many metal superhydrides with a lighter ion and more hydrogen present (e.g., LiH_x) [24] exhibit a lower T_c than La and Y superhydrides. On the other hand, YH_{10} and MgH_6 are computed to have a higher T_c than LaH_{10} and CaH_6, respectively, but the lighter ions require higher pressures to attain their maximum T_c values. The lighter metal atoms exhibit lower frequency vibrational modes, conducive for superconductivity, and higher electron-phonon coupling, influenced by the weak multicentered hydrogen bonding, although the exact nature of the periodic trends remains to be seen.

Herein, we present an alternative technique to overcome many of the hurdles inhibiting the synthesis of metal superhydrides in a diamond anvil cell. Using the technique of coating the target metal (yttrium) with a thin film of palladium—a metal known to promote hydrogenation, we report the discovery of superconductivity in an

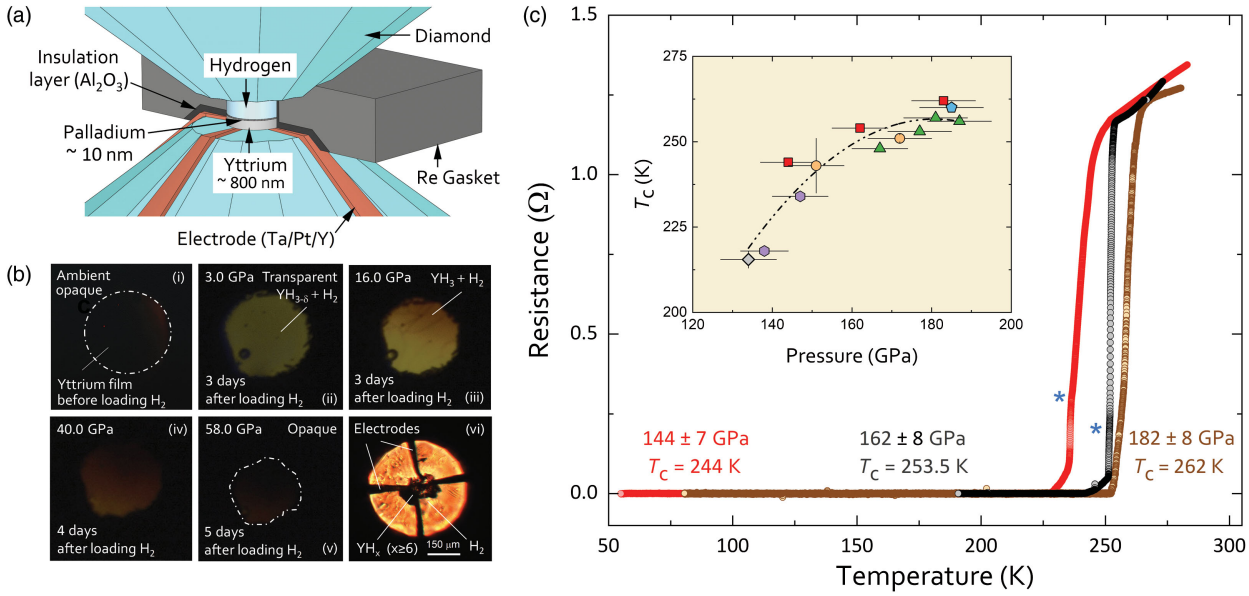

FIG. 1. (a) Schematic of a new experimental approach for the preparation of metal films for the synthesis of metal superhydrides. (b) Microphotographs from transmitted light of yttrium film in a hydrogen environment. (i) and (ii) When initially opaque yttrium film is exposed to H_2 gas, it readily absorbs hydrogen and forms metallic stoichiometric dihydride ($YH_{2\pm\epsilon}$) and, eventually, nonmetallic, hcp trihydride ($YH_{3\pm\delta}$ with $\delta \simeq 0.2$) at low pressure. When the mixture of $YH_{3\pm\delta}$ and H_2 is further pressurized (to about 5 GPa), fully transparent and yellowish YH_3 is synthesized. However, the transmission shifts toward the red (iii) and (iv) above 15 GPa, and eventually the sample again becomes completely opaque to the visible spectrum (v) above 60 GPa at ambient temperature. (vi) Illustrates the synthesized superhydride sample (YH_x: $x \geq 6 + H_2$) with electrical leads for resistance measurements. (c) Temperature-dependent electrical resistance of yttrium superhydride at high pressures, showing the superconducting transition is as high as 262 K at 182 ± 8 GPa, the highest pressure measured in this experimental run. The data were obtained during the warming cycle to minimize the electronic and cooling noise. Inset: The pressure dependence of the T_c as determined by a sharp drop in electrical resistance, showing the increase in T_c with pressure and plateau around 175 GPa, approaching a dome shape. The colors represent different experiments.

yttrium superhydride with a maximum T_c of 262 K at 182 ± 8 GPa. Comparison of the measured T_c with theoretical estimates based upon Bardeen-Cooper-Schrieffer (BCS) theory, and the observed Raman spectra with results obtained from first-principles calculations suggest that the superconductivity arises from a clathrate phase with stoichiometry close to YH_9 [14,16–19].

Yttrium and the trivalent rare-earth elements are extremely reactive, which makes them difficult to study [25]. To overcome these difficulties, we employed a nonconventional synthesis technique in a diamond anvil cell (DAC)—sputtering an yttrium film (400 to 800 nm) in the middle of the diamond culet under high vacuum and coating it with a thin layer of palladium (10 ± 5 nm) [Fig. 1(a)]. Palladium is a noble metal with a well-known ability to catalyze hydrogenation, hydrogen purification, and hydrogen storage by promoting uptake of hydrogen into its lattice then transferring it to other materials [26]. Palladium accomplishes this by dissociating molecular hydrogen and incorporating the hydrogen atoms into octahedral sites of the fcc Pd lattice (β-PdH_x). The predissociation of molecular hydrogen by palladium thin films along with its high hydrogen transport [27], has already been shown to catalyze yttrium and lanthanum metals into $REH_{3-\delta}$ at 300 K and 9×10^5 Pa of H_2 in a matter of minutes [28]. Using our setup [Fig. 1(a)] akin to that of Huiberts *et al.* [28], we were able to fully transform a sputtered yttrium sample to YH_3 in a DAC over a period of ~18 h at 4.5 GPa at room temperature without any other external stimuli [Fig. 1(b)]. To evaluate the efficacy of Pd thin film hydrogenation, DACs were prepared without either the Y or Pd component, and using sputtered samples vs thin foils. The Y only DAC exhibited incomplete synthesis, and the Pd thin film only DAC showed no detectable change. This procedure ensures that our starting material for a high pressure yttrium superhydride synthesis is YH_3. Starting with the trihydride is advantageous over other approaches as it provides a higher initial hydrogen content than direct elemental combination, and it avoids using chemical precursors as a source of hydrogen (e.g., ammonia borane), which very likely leads to contamination beyond a pure binary system.

To synthesize the yttrium superhydride, the dense, film-coated YH_x ($x \geq 3$) and H_2 are compressed above 130 GPa and directly heated by a V-GEN Yb Pulsed Fiber Laser at 1064 nm [Fig. 1(b)]. The estimated lower bound of the temperature of the samples during heating is 1800 K. The Pd should be stoichiometric (or near) β-PdH_x by 100 GPa, and laser heating removes all barriers to hydrogen diffusion through β-PdH_x [29]. Thus, we believe that the laser heated

Pd is again acting to catalyze the formation of the superhydride by removing the barriers associated with dissociating molecular H_2 and driving the transport of H to the yttrium system. This method permits a facile transformation pathway for metal superhydride materials predicted to have high T_cs.

The synthesized yttrium superhydride has a maximum superconducting transition temperature of 262 K at 182 ± 8 GPa, as is evident by a sharp drop in resistance over a 5° to 10° temperature change [Fig. 1(c)]. Further more, all the yttrium superhydride samples prepared using this technique exhibit a high T_c immediately postlaser heating at high pressure. The transition temperature increases with pressure from 216 K at 134 ± 5 GPa until it plateaus around 175 GPa, which is then followed by a slight decrease approaching a dome shape [Fig. 1(c) inset]. At 144 GPa, the superconducting transition is signified by two sharp resistance drops: a very large (≈75%) drop that occurs relatively slowly ($\Delta T = 8$ K) at around 244 K, and a small (≈25%) but sharp ($\Delta T < 1$ K) drop at around 237 K [indicated by * in Fig. 1(c)]. A similar behavior is also observed at one of the highest pressures measured, 182 ± 8 GPa, with the 262 K transition. These pressures are measured using the H_2 vibron scale, but it should be noted that pressures measured from the diamond edge using the Akahama 2006 scale [30] are at least 10% to 12% higher. The transition temperatures were taken from the onset of superconductivity using a probe with ±0.1 K accuracy, where the resistance is measured during the natural warming cycle (≈0.25 K/min) from low temperature with a current of 10 μA to 1 mA.

To investigate the isotope effect, D_2 replaced H_2 in the experimental setup and yttrium superdeuteride samples were synthesized at the same conditions as the superhydrides. The substitution of deuterium noticeably affects the value of the T_c, which shifts to lower temperatures, indicating phonon-assisted superconductivity (Fig. 2). The isotopic shift in critical temperature is expected to scale as $\propto m^{-\alpha}$, with m being the atomic mass and α the isotope coefficient. A strong isotope effect is observed at 177 GPa with $T_c = 256$ K for yttrium superhydride and $T_c = 183$ K for the superdeuteride. The isotope coefficient obtained from those measurements is $\alpha = -[\ln T_c(YD_x) - \ln T_c(YH_x)]/\ln 2 = 0.48$, in very good agreement with the BCS value of $\alpha \approx 0.5$ for conventional superconductivity.

Our typical yttrium superhydride samples are 30–50 μm in diameter, making it almost impossible to search for the Meissner effect in the dc magnetization or even the shielding effect in the dc or ac magnetic susceptibility [31,32]. These difficulties signal the need for novel experimental capabilities [33–36], but an alternative method to confirm a superconducting transition at high pressure exploits the inherent hostility of an external magnetic field on superconductivity. The upper critical field H_c is the maximum external magnetic field that

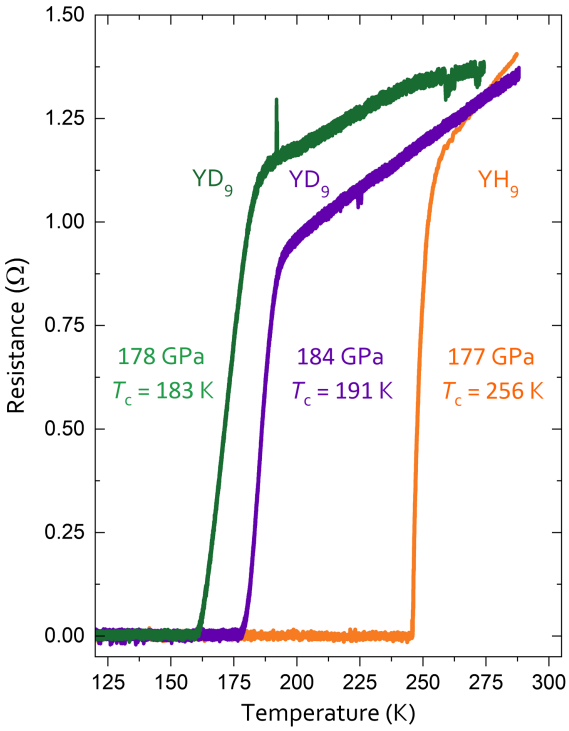

FIG. 2. The substitution of hydrogen with deuterium noticeably affects the value of T_c, which shifts to 183 K at 177 GPa. The calculated isotope coefficient at 177 GPa with $T_c = 256$ K for $YH_{9\pm x}$ (orange curve) and $T_c = 183$ K for the $YD_{9\pm x}$ (green curve) sample is 0.48. By comparing the transition temperatures at around 183 GPa, we obtained $\alpha = 0.46$. Both values are in very good agreement with the Bardeen-Cooper-Schrieffer value of $\alpha = 0.5$ for conventional superconductivity.

superconductivity can survive. This value is controlled by both the paramagnetic effect of electron spin polarization due to the Zeeman effect and the diamagnetic effect of orbital motion of the Cooper pairs due to the Lorentz force. Under an applied magnetic field, these effects combine to reduce the T_c. In the present studies, application of an external magnetic field reduces T_c by about 14 K at 6 T and 177 GPa (Fig. 3), confirming the superconducting transition. The upper critical field, formula $H_c(T) = H_c(0)[1 - (T/T_c)^2]$, in the 0 K limit is 103.2 T (Fig. 3, top inset). The field dependence of the superconducting transition width, ΔT_c, at 177 GPa is linear (Fig. 3, bottom inset) as is expected from the percolation model. ΔT_c is defined here as $\Delta T_c = T_{90\%} - T_{10\%}$, where $T_{90\%}$ and $T_{10\%}$ are the temperatures corresponding to 90% and 10% of the resistance at 260 K at 177 GPa. Fitting to $\Delta T_c = \Delta T_c(0) + kH$ gives a transition width at zero external field $\Delta T_c(0) = 7.62$ K and proportionality constant $k = 0.07$ KT^{-1}. Such a large $\Delta T_c(0)$ indicates sample inhomogeneities, which is typical for DAC experiments. For instance, the transition width for LaH_{10} is 7.3 K and H_3S can vary from 5.5 to 26 K [9,32,37].

There have been moderate differences between the high T_c responses of the RE superhydrides reported [31,32,38].

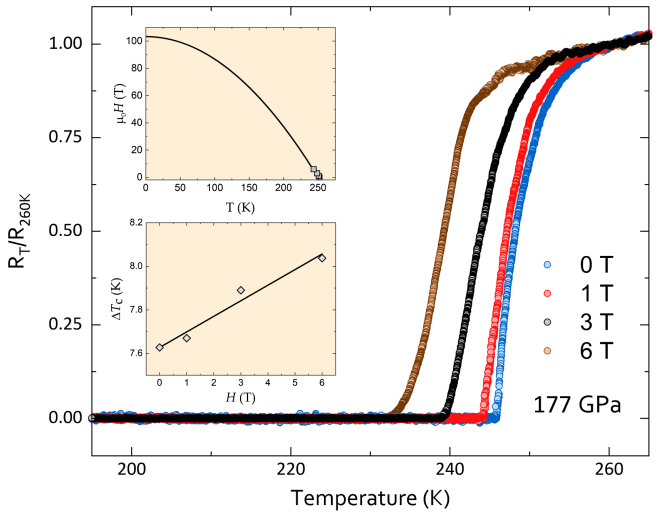

FIG. 3. Superconducting transition under an external magnetic field. Low-temperature electrical resistance behavior under a magnetic field of H = 0, 1, 3, and 6 T (increasing from right to left) at 177 GPa. Pressure was determined by the hydrogen vibron position. Inset top: Upper critical field vs temperature. An extrapolation to the lowest temperature yields 103.2 T for the upper critical magnetic field in the limit of zero temperature. Inset bottom: Superconducting transition width, ΔT_c, as a function of H, showing a linear relationship.

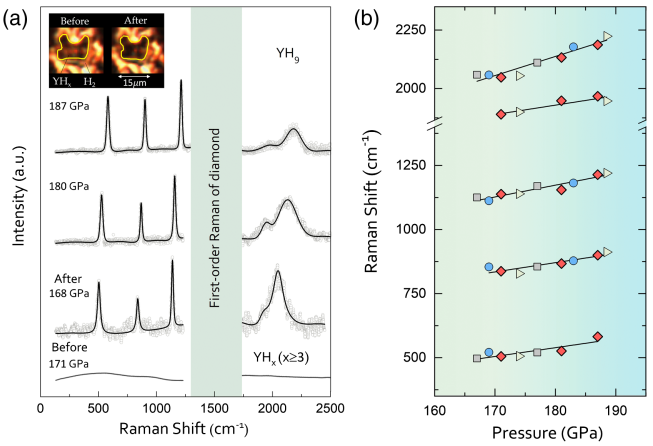

FIG. 4. Synthesis of yttrium superhydride at high pressures and high temperatures. (a) Pressure-induced Raman changes (background subtracted) of yttrium superhydride for several indicated pressures at room temperature. Before heating (bottom spectra), the pressure was 171 GPa; after heating, it dropped to 168 GPa, suggesting a volume collapse associated with the transition. The observed characteristic Raman modes of the new material are in good agreement with theoretical calculations for YH_9 (Fig. S9). The peak around 2048 cm^{-1} is broad compared to the low-frequency peaks, and there may be a shoulder at 1890 cm^{-1}. The shaded area corresponds to the strong diamond signal. Inset: Microphotographs of transmitted light of the sample before and after heating. For clarity we have included a line (yellow) around the boundary of the sample. The sample became darker after heating to above 1800 K. (b) Pressure-induced Raman shift of different vibrations of the new yttrium superhydride. The colors indicate different experiments.

Most relevant is our higher T_c of nearly 20 K, compared to Kong *et al.* [38]. The potential of the presence of mixed phases present in either this study or any of the other metal superhydride phases reported cannot be excluded. However, the superconducting response measured is most likely from a single phase that is above the necessary phase fraction for bulk conductivity measurements. It is important to note that the abundance of the phase fractions will be defined by the percolation of the new thermodynamically stable phase and any kinetic barriers on the pathway. The use of a chemical precursor for a source of hydrogen vs elemental starting materials or the specific reaction pathway can also effect the final state measured. Alternatively, the synthesized superhydride materials could have defects in the lattice where H differs from the ideal stoichiometry, i.e., $YH_{9\pm x}$. This is a known issue in lower H-content yttrium hydrides, for instance the formation of $YH_{2.86}$ at near ambient pressures in the earlier Pd film work [28]. Such subtle changes in these systems must be probed by spectral techniques beyond diffraction that are sensitive to the local atomistic coordination environments.

Raman scattering is a spectral technique that is highly sensitive to the bonding environment of materials, and Fig. 4 shows Raman spectra that were obtained before and after pulsed heating of a mixture of dense YH_x ($x \geq 3$) and H_2 at 171 GPa. The changes in the spectra signify that the sample transforms to an entirely new structure upon laser heating. Before heating, the Raman spectra of the sample is featureless, and the spectrum postheating has three, sharp, characteristic Raman peaks around 505, 833, and 1136 cm^{-1} and a broad peak at 2048 cm^{-1}. The broad peak contains a shoulder at 1890 cm^{-1} (Fig. 4). After several cycles of pulsed laser heating, a reasonable pressure drop (1%–2% of the initial pressure) is observed. The drop suggests a volume collapse is associated with the transition to the superhydride.

Comparison of the measured Raman spectrum at 187 GPa [Fig. S9(a) top] with the ones computed for various YH_n phases (Fig. S7) at 190 GPa [Fig. S7(b)] immediately shows that the experimental results cannot be explained by $Im\bar{3}m$ YH_6 (because its only Raman active mode is within the diamond zone), nor a nonmetallic $P6_3/m$ symmetry YH_9 (because it has an intense peak at 3630 cm^{-1} due to the H_2 vibron). Considering that the computational methodology employed is likely to underestimate the vibrational frequencies by approximately 240 cm^{-1} (Fig. S5), the YH_{10} mode computed to lie at 1703 cm^{-1} could potentially account for the broad shoulder observed at 2200 cm^{-1}. However, YH_{10} only has two modes whose frequencies fall below that of the diamond mode, whereas experiment observes three centered at 582, 899, and 1221 cm^{-1}. Turning to the $P6_3/mmc$ YH_9 clathrate phase, we observe good agreement between the calculated and observed spectrum at three different

pressures (Fig. S9), especially considering that within the pressure range considered our computational methodology underestimated the H_2 vibron by 243 cm^{-1}. We postulate that the broadening due to quantum nuclear effects [39] is particularly important for the high frequency modes above 1500 cm^{-1}, which could merge into a single peak with a pronounced shoulder similar to what is observed experimentally. A comparison of the experimental and theoretical frequencies of the major peaks vs pressure plots (Fig. S9) is also in good agreement, especially taking into account that the theoretical results are likely too low. We also calculated the Raman spectrum of $P6_3/mmc$ YD_9 at 180 GPa and compared the results with experiment (Fig. S10). The calculated and measured peak positions are in excellent agreement with each other, however we overestimate the intensity of the mode centered at 949 cm^{-1}. Our results show that we have successfully synthesized an yttrium superhydride material at high pressure and elevated temperatures which we tentatively assign as $YH_{9\pm x}$.

In conclusion, Pd catalyzed hydrogenation of sputtered yttrium produced an yttrium superhydride with a maximum superconducting transition temperature of 262 K at 182 ± 8 GPa. Analysis using Raman spectroscopy reveals a uniform material with similar features to a YH_9 clathrate structure but with some subtle differences, leading us to conclude that we have synthesized $YH_{9\pm x}$. Despite extensive efforts, we do not observe room-temperature superconductivity up to the highest pressure studied, therefore the search for RTSC in these metal superhydrides remains open. Based on the strong isotope effect, the mechanism of pairing is convincingly conventional, but further research is needed for a complete understanding of the underlying mechanism in this new class of quantum materials.

We thank Lilia Boeri for providing the preliminary calculated Raman frequencies of yttrium superhydrides, Hiranya Pasan for reanalyzing the low temperature data, Desmond Wentling for his technical support during the initial stage of the project, and Dean Smith for useful discussions and technical support. Also, we thank Ori Noked, Christian Koelbl, and Lauren Koelbl for useful discussions. We thank Brian McIntyre and James Mitchell for their technical support on the preparation of diamond surfaces at the University of Rochester Integrated Nanosystems Center. Calculations were performed at the Center for Computational Research at SUNY Buffalo [40]. This research was supported by NSF, Grant No. DMR-1809649, and DOE Stockpile Stewardship Academic Alliance Program, Grant No. DE-NA0003898. This work was supported by the U.S. Department of Energy, Office of Science, Fusion Energy Sciences under Award No. DE-SC0020340. A. S. and K. V. L. acknowledges support from U.S. Department of Energy, Office of Basic Energy Sciences under No. DE-SC0020303. X. W. and E. Z. acknowledge NSF Grant No. DMR-1827815.

*rdias@rochester.edu
†These contributed equally to this work.

[1] N. W. Ashcroft, Phys. Rev. Lett. **21**, 1748 (1968).
[2] S. A. Bonev, E. Schwegler, T. Ogitsu, and G. Galli, Nature (London) **431**, 669 (2004).
[3] J. M. McMahon and D. M. Ceperley, Phys. Rev. Lett. **106**, 165302 (2011).
[4] J. McMinis, R. C. Clay, D. Lee, and M. A. Morales, Phys. Rev. Lett. **114**, 105305 (2015).
[5] R. P. Dias and I. F. Silvera, Science **355**, 715 (2017).
[6] M. Zaghoo, A. Salamat, and I. F. Silvera, Phys. Rev. B **93**, 155128 (2016).
[7] V. Struzhkin, B. Li, C. Ji, X.-J. Chen, V. Prakapenka, E. Greenberg, I. Troyan, A. Gavriliuk, and H.-K. Mao, Matter Radiat. Extremes **5**, 28201 (2020).
[8] B. Stritzker and H. Wühl, in *Hydrogen in Metals II: Application-Oriented Properties*, edited by G. Alefeld and J. Völkl (Springer, Berlin, Heidelberg, 1978), pp. 243–272.
[9] A. P. Drozdov, M. I. Eremets, I. A. Troyan, V. Ksenofontov, and S. I. Shylin, Nature (London) **525**, 73 (2015).
[10] D. Duan, Y. Liu, F. Tian, D. Li, X. Huang, Z. Zhao, H. Yu, B. Liu, W. Tian, and T. Cui, Sci. Rep. **4**, 6968 (2014).
[11] J. J. Hamlin, Physica (Amsterdam) **514C**, 59 (2015).
[12] I. Errea, M. Calandra, C. J. Pickard, J. R. Nelson, R. J. Needs, Y. Li, H. Liu, Y. Zhang, Y. Ma, and F. Mauri, Nature (London) **532**, 81 (2016).
[13] E. Snider, N. Dasenbrock-Gammon, R. McBride, M. Debessai, H. Vindana, K. Vencatasamy, K. V. Lawler, A. Salamat, and R. P. Dias, Nature (London) **586**, 373 (2020).
[14] F. Peng, Y. Sun, C. J. Pickard, R. J. Needs, Q. Wu, and Y. Ma, Phys. Rev. Lett. **119**, 107001 (2017).
[15] N. W. Ashcroft, Phys. Rev. Lett. **92**, 187002 (2004).
[16] H. Liu, I. I. Naumov, R. Hoffmann, N. W. Ashcroft, and R. J. Hemley, Proc. Natl. Acad. Sci. U.S.A. **114**, 6990 (2017).
[17] A. R. Oganov, C. J. Pickard, Q. Zhu, and R. J. Needs, Nat. Rev. Mater. **4**, 331 (2019).
[18] E. Zurek and T. Bi, J. Chem. Phys. **150**, 050901 (2019).
[19] J. A. Flores-Livas, L. Boeri, A. Sanna, G. Profeta, R. Arita, and M. Eremets, Phys. Rep. **856**, 1 (2020).
[20] Y. Quan, S. S. Ghosh, and W. E. Pickett, Phys. Rev. B **100**, 184505 (2019).
[21] C. Heil, S. di Cataldo, G. B. Bachelet, and L. Boeri, Phys. Rev. B **99**, 220502(R) (2019).
[22] I. Errea, F. Belli, L. Monacelli, A. Sanna, T. Koretsune, T. Tadano, R. Bianco, M. Calandra, R. Arita, F. Mauri, and J. A. Flores-Livas, Nature (London) **578**, 66 (2020).
[23] X. Ye, N. Zarifi, E. Zurek, R. Hoffmann, and N. W. Ashcroft, J. Phys. Chem. C **122**, 6298 (2018).
[24] Y. Xie, Q. Li, A. R. Oganov, and H. Wang, Acta Crystallogr., Sect. C **70**, 104 (2014).
[25] NOAA, Chemical Datasheet-Yttrium; NOAA and Environmental Protection Agency CAMEO Chemicals database.
[26] B. D. Adams and A. Chen, Mater. Today **14**, 282 (2011).
[27] S. Dekura, H. Kobayashi, K. Kusada, and H. Kitagawa, ChemPhysChem **20**, 1158 (2019).

[28] J. N. Huiberts, R. Griessen, J. H. Rector, R. J. Wijngaarden, J. P. Dekker, D. G. de Groot, and N. J. Koeman, Nature (London) **380**, 231 (1996).
[29] B. Guigue, G. Geneste, B. Leridon, and P. Loubeyre, J. Appl. Phys. **127**, 075901 (2020).
[30] Y. Akahama and H. Kawamura, J. Appl. Phys. **100**, 043516 (2006).
[31] M. Somayazulu, M. Ahart, A. K. Mishra, Z. M. Geballe, M. Baldini, Y. Meng, V. V. Struzhkin, and R. J. Hemley, Phys. Rev. Lett. **122**, 027001 (2019).
[32] A. P. Drozdov, P. P. Kong, V. S. Minkov, S. P. Besedin, M. A. Kuzovnikov, S. Mozaffari, L. Balicas, F. F. Balakirev, D. E. Graf, V. B. Prakapenka, E. Greenberg, D. A. Knyazev, M. Tkacz, and M. I. Eremets, Nature (London) **569**, 528 (2019).
[33] I. Troyan, A. Gavriliuk, R. Rüffer, A. Chumakov, A. Mironovich, I. Lyubutin, D. Perekalin, A. P. Drozdov, and M. I. Eremets, Science **351**, 1303 (2016).
[34] F. Capitani, B. Langerome, J.-B. Brubach, P. Roy, A. Drozdov, M. I. Eremets, E. J. Nicol, J. P. Carbotte, and T. Timusk, Nat. Phys. **13**, 859 (2017).
[35] S. Hsieh, P. Bhattacharyya, C. Zu, T. Mittiga, T. J. Smart, F. MacHado, B. Kobrin, T. O. Höhn, N. Z. Rui, M. Kamrani, S. Chatterjee, S. Choi, M. Zaletel, V. V. Struzhkin, J. E. Moore, V. I. Levitas, R. Jeanloz, and N. Y. Yao, Science **366**, 1349 (2019).
[36] M. Lesik, T. Plisson, L. Toraille, J. Renaud, F. Occelli, M. Schmidt, O. Salord, A. Delobbe, T. Debuisschert, L. Rondin, P. Loubeyre, and J.-F. Roch, Science **366**, 1359 (2019).
[37] S. Mozaffari, D. Sun, V. S. Minkov, A. P. Drozdov, D. Knyazev, J. B. Betts, M. Einaga, K. Shimizu, M. I. Eremets, L. Balicas, and F. F. Balakirev, Nat. Commun. **10**, 2522 (2019).
[38] P. P. Kong *et al.*, arXiv:1909.10482.
[39] L. Monacelli, I. Errea, M. Calandra, and F. Mauri, Nat. Phys. **17**, 63 (2021).
[40] Center for Computational Research. CCR Facility Description, http://hdl.handle.net/10477/79221.
[41] See Supplemental Material at http://link.aps.org/supplemental/10.1103/PhysRevLett.126.117003 for materials and methods, high pressure studies of palladium and hydrogen mixture, hydrogenation Process, Raman spectra calculations using DFPT, computed Raman spectra of various YHn phases, and compiled details of experimental runs.